Toxicology in Vitro 27 (2013) 323–329

Contents lists available at SciVerse ScienceDirect

Toxicology in Vitro

journal homepage: www.elsevier.com/locate/toxinvit

Toxicity of terpenes on fibroblast cells compared to their hemolytic potential and increase in erythrocyte membrane fluidity

Sebastião A. Mendanha [a], Soraia S. Moura [b], Jorge L.V. Anjos [a], Marize C. Valadares [b], Antonio Alonso [a,*]

[a] Instituto de Física, Universidade Federal de Goiás, Goiânia, GO, Brazil
[b] Laboratório de Farmacologia e Toxicologia Celular – FARMATEC, Faculdade de Farmácia, Universidade Federal de Goiás, Goiânia, GO, Brazil

ARTICLE INFO

Article history:
Received 4 May 2012
Accepted 16 August 2012
Available online 27 August 2012

Keywords:
EPR
Spin label
Toxicity
Fibroblast
Terpenes
Erythrocyte membrane

ABSTRACT

Terpenes are considered potent skin permeation enhancers with low toxicity. Electron paramagnetic resonance (EPR) spectroscopy of the spin label 5-doxyl stearic acid (5-DSA) was used to monitor the effect of sesquiterpene nerolidol and various monoterpenes on membrane fluidity in erythrocyte and fibroblast cells. In addition, the hemolytic levels and cytotoxic effects on cultured fibroblast cells were also measured to investigate possible relationships between the cellular irritation potentials of terpenes and the ability to modify membrane fluidity. All terpenes increased cell membrane fluidity with no significant differences between the monoterpenes, but the effect of sesquiterpene was significantly greater than that of the monoterpenes. The IC_{50} values for the terpenes in the cytotoxicity assay indicated that 1,8-cineole showed lower cytotoxicity and α-terpineol and nerolidol showed higher cytotoxicity. The correlation between the hemolytic effect and the IC_{50} values for fibroblast viability was low ($R = 0.61$); however, in both tests, nerolidol was among the most aggressive of terpenes and 1,8-cineole was among the least aggressive. Obtaining information concerning the toxicity and potency of terpenes could aid in the design of topical formulations optimized to facilitate drug absorption for the treatment of many skin diseases.

1. Introduction

Terpenes are volatile constituents of the essential oils of citrus fruits, cherries, mints and herbs that contain only carbon, hydrogen and oxygen atoms. They can be chemically classified as alcohols, hydrocarbons, ketones and epoxides. Physiologically, terpenes function primarily as chemoattractants or chemorepellents (McGarvey and Croteau, 1995) and are largely responsible for the characteristic fragrance of many plants (Crowell, 1999). Recently, the potential of terpenes as potent skin permeation enhancers for drug delivery systems has received considerable attention, especially because they are naturally occurring substances with low skin irritation. Many terpenes, including 1,8-cineole, menthol and α-terpineol, are included on the list of "Generally Recognized As Safe" (GRAS) materials. Several monoterpenes show no change or only a slight irritation and cytotoxic effect on cultured human skin cells (Kitahara et al., 1993). In this context, skin permeation enhancers, particularly oxygen-containing terpenes, were used as accelerants of permeation for lipophilic drugs, such as 5-fluorouracil (Cornwell and Barry, 1994), morphine (Morimoto et al., 2002), imipramine (Jain et al., 2002), hydrocortisone (El-Kattan et al., 2000) and haloperidol (Vaddi et al., 2002).

A number of dietary monoterpenes have demonstrated antitumor activity and are effective in the chemoprevention and chemotherapy of cancer (Crowell, 1999; Rabi and Bishayee, 2009; Thoppil and Bishayee, 2011; Gould, 1997; Bardon et al., 1998, 2002; Wu et al., 2012; Yang and Ping Dou, 2010; Polo and de Bravo, 2006). The monoterpenes linalool, carvacrol, geraniol and terpinen-4-ol have shown activity against Leishmania *infantum* promastigotes (Morales et al., 2009). Moreover, terpinen-4-olo and the sesquiterpene nerolidol were reported to show antifungal (Oliva et al., 2003) and antileishmanial activity (Arruda et al., 2005), respectively.

Electron paramagnetic resonance (EPR) spectroscopy of spin labels has been recently used to investigate the mechanisms underlying the action of terpenes as accelerants of skin permeation. The intercellular membranes of the stratum corneum, which is the outermost skin layer and primary physical barrier for skin permeation, become fluid in presence of the terpenes L-menthol (Dos Anjos et al., 2007) and 1,8-cineole (Anjos et al., 2007). In addition, treatment with monoterpenes increases the partition coefficient of the small water-soluble spin labels TEMPO (Dos Anjos and Alonso, 2008) and DTBN (Camargos et al., 2010) into stratum corneum membranes. These results suggest that terpenes might effectively act as spacers in the membrane to fluidize lipids and create

Abbreviations: EPR, electron paramagnetic resonance; 5-DSA, 5-doxyl stearic acid.

* Corresponding author. Fax: +55 62 3521 1014.
E-mail address: alonso@if.ufg.br (A. Alonso).

0887-2333
http://dx.doi.org/10.1016/j.tiv.2012.08.022

ruptures in the hydrogen-bond network of the polar interface (Dos Anjos and Alonso, 2008).

Few studies have investigated whether the ability of terpenes to facilitate chemical absorption correlates with increased irritation potentials. Terpenes are important skin permeation enhancers for drug delivery systems; therefore, we investigated the effect of nerolidol, α-terpineol, L(−)-carvone, (+)-limonene, L-menthone, DL-menthol, pulegone and 1,8-cineole on erythrocyte membrane fluidity. Moreover, the hemolytic potentials and toxicity levels of these terpenes on fibroblast cells were also investigated.

2. Materials and methods

2.1. Chemicals and preparation

Materials for the 3T3 Neutral Red Uptake (NRU) assay and the spin label 5-doxyl stearic acid (5-DSA) (Fig. 1) were purchased from Sigma–Aldrich (St. Louis, MO, USA; Steinheim, Germany). The terpenes were purchased from Acros Organics (Geel, Belgium). All other chemicals were of the highest grade available and the buffers were prepared with Milli-Q water.

2.2. Cell culture

Balb/c 3T3-A31 fibroblasts were cultured in Dulbecco's Modified Eagle's Medium (DMEM – D5648 Sigma–Aldrich), supplemented with 10% fetal bovine serum (FBS-GIBCO) at 37 ± 1 °C, 90 ± 10% humidity, 5.0 ± 1.0% CO_2/air. The cells were removed from the culture flasks using trypsinization (trypsin:EDTA solution at a 0.25%:0.02% ratio) when they exceeded 50% confluence but prior to reaching 80% confluence. Cell viability was evaluated using the Trypan blue exclusion method with a Neubauer chamber.

A cell suspension containing 3×10^4 cells/mL was prepared on the day of plate seeding using culture medium supplemented with 10% FBS. The peripheral wells (blanks) of the 96-well microtiter plates were seeded with 100 μL of routine culture medium and the remaining wells received 100 μL of a suspension containing 3×10^4 cells/mL (3×10^3 cells/well). The plates were incubated for 24 ± 2 h (37 ± 1 °C; 90 ± 10% humidity, 5.0 ± 1.0% CO_2/air) to allow the cells to form a monolayer of less than 50% confluence. This incubation period assured cell recovery, adherence and progression to the exponential growth phase. Each plate was examined under a phase contrast microscope to identify experimental and systemic cell seeding errors.

2.3. The Neutral Red Uptake (NRU) assay

For *in vitro* assays, the terpenes (nerolidol, α-terpineol, L(−)-carvone, (+)-limonene, L-menthone, DL-menthol, pulegone or 1,8-cineole) were prepared individually as a micellar suspension to allow dissolution in water. The micelles were prepared as follows: 10 mg of phosphatidylcholine (PC) and 50 μL of the terpenes to be tested were dissolved in 50 μL of ethanol. The mixture was sonicated for 10 min in a Ti-probe sonicator to obtain a homogeneous dispersion of small micelles. The micellar suspension was prepared without terpenes for control groups. The experimental samples were directly diluted in culture medium (DMEM) to obtain the concentration of use and filtered through a syringe-filter with a PES TPP® membrane (0.22 μm pore size) to assure sterility. The final concentration of ethanol in all cultures was lower than 0.05%.

A Balb/c 3T3-A31 cell suspension containing 3×10^4 cells/well was seeded in 96-well plates, and after a 24 h recovery period, the plates were treated with eight different concentrations of freshly prepared test compounds in complete medium (six wells per concentration) and incubated for an additional 48 h. The control wells (blanks) received complete culture medium supplemented with 10% FBS. Subsequently, 250 μL of neutral red (NR) medium was added to all wells, including the blanks, and incubated (37 ± 1 °C, 90 ± 10% humidity, 5.0 ± 1.0% CO_2/air) for 3.0 ± 0.1 h. The cells were briefly observed 2–3 h after incubation for NR crystal formation. After 3 h, the NR medium was removed and the cells were carefully rinsed with 250 μL/well of pre-warmed PBS. The PBS was decanted from the plate and 100 μL of NR desorb (50:1:49 EtOH:acetic acid:water) solution was added to all wells, including the blanks. The plates were rapidly shaken on a microplate shaker for 20 min to extract the NR. The absorption was measured at 545 nm in a microtiter plate reader (spectrophotometer). The optical density (OD) was calculated as the difference between the absorbances at the test wavelength and that at the reference wavelength. For each concentration tested, the wells containing no cells served as reference blanks.

2.4. Blood processing

The blood samples, obtained from three donors of two blood banks, were diluted in PBS and centrifuged at 150*g* for 10 min at 4 °C. The plasma and white cells were carefully removed after each wash (three times).

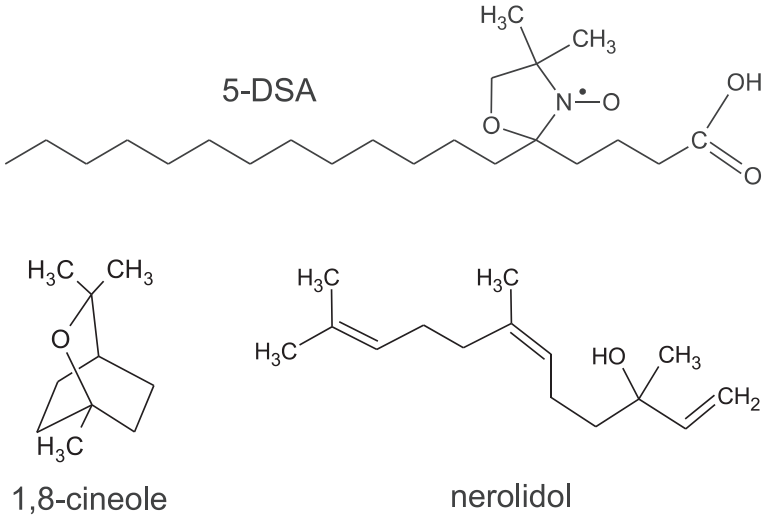

Fig. 1. The chemical structures of two terpenes and the spin label 5-DSA used in this work.

2.5. Hemolytic induction

To induce hemolysis, aliquots of terpenes diluted in ethanol (300 mM) were added to tubes containing erythrocytes suspended in PBS at a hematocrit concentration of 50% (final volume of 100 μL). After gentle shaking, the tubes were incubated at 37 °C for 1.5 h. Subsequently, the erythrocytes were precipitated by centrifugation at 300*g* and 25 °C for 10 min. The magnitude of hemolysis was determined spectrophotometrically at 540 nm according to the equation:

$$\%\text{hemolysis} = \frac{A_a - A_{c1}}{A_{c2} - A_{c1}}$$

where A_{c1} is the control sample (0% terpene), A_{c2} is the completely hemolyzed sample in Milli-Q water and A_a is the sample containing the desired terpene concentration. Terpene concentration that causes 50% hemolysis was determined in units of mM. It is well known that an average human erythrocyte occupies a volume of approximately 90 fL. The number of cells in the sample and the ratio of terpenes/cell for 50% hemolysis were calculated based on this volume.

2.6. Erythrocyte and fibroblast membranes labeling and terpene treatments

The terpenes were dissolved in ethanol to the desired concentration, and 4 μL of the solution was applied directly to the cell suspension (45 μL). The terpene-erythrocyte or terpene-fibroblast suspensions were incubated at 37 °C for 1.5 h. Subsequently, a small aliquot (~1 μL) of the spin label 5-DSA (Fig. 1) dissolved in ethanol (5 mg/mL) was added to the cells. Each sample consisting of 5.0×10^8 RBCs or 1.3×10^7 fibroblasts in PBS containing 10% ethanol and the desired terpene concentration was introduced in capillary tube and flame-sealed for the EPR measurement. Control samples, with and without ethanol, were measured and it was found that this concentration of ethanol did not significantly alter the membrane fluidity in either RBC or fibroblast cells. In calculating the ratio of terpene molecules/cell for each sample, the erythrocyte volume was considered to be 90 fL and for fibroblast samples the number of cells was counted.

2.7. EPR spectroscopy

The EPR spectra were recorded using a Bruker ESP 300 spectrometer (Rheinstetten, Germany) equipped with an ER 4102 ST resonator. The instrument was programmed with the following settings: microwave power, 2 mW; modulation frequency, 100 kHz; modulation amplitude, 1.0 G; magnetic field scan, 100 G; sweep time, 168 s; and detector time constant, 41 ms. All measurements were performed at room temperature (24–26 °C). The EPR spectra simulations were performed using nonlinear least-square (NLLS) fits and the general slow-motion program (Schneider and Freed, 1989; Budil et al., 1996). The rotational diffusion rate, R_{bar}, obtained from NLLS was converted to the rotational correlation time, τ_c, through the relationship $\tau_c = 1/6\ R_{bar}$ (Schneider and Freed, 1989). Similar to previous studies (Alonso et al., 2001, 2003; Queirós et al., 2005), the magnetic parameters were determined based on the global analysis of the overall spectra obtained in this work, and all of the EPR spectra were simulated using the same predetermined parameters. The magnetic *g* and *A* tensors are defined in a molecule-fixed frame, where the constants of rotational diffusion rates around the *x*, *y* and *z* axes are included. The input parameters of tensors *g* and *A* were: $g_{xx} = 2.0088$; $g_{yy} = 2.0060$; $g_{zz} = 2.0026$; $A_{xx} = 6.1$; $A_{yy} = 6.3$ G; $A_{zz} = 36.5$ G.

2.8. Statistical analysis

Data from the microtiter plate reader were transferred to a spreadsheet template GraphPad Prism® to determine the cell viability, calculate the IC_{50} values using linear interpolation, and perform the statistical analyses.

Concentration–response curves were constructed and fitted in ®Origin 8.0 using parametric nonlinear regression. IC_{50} values were computed using the fitted Hill equation and presented as the mean ± standard deviation (SD) of at least three independent experiments with 4 repetitions in each experiment (12 experimental values for each compound). IC_{50} data were compared by one-way analysis of variance (ANOVA) followed by Tukey's multiple range test for statistically significant differences at $P < 0.05$.

3. Results

3.1. Cytotoxicity of the terpenes

In the present study we used the 3T3 NRU to evaluate the cytotoxicity of eight terpenes. The results were obtained for different concentrations of terpenes in a Balb/c 3T3-A31 NRU cytotoxicity assay after incubation for 48 h. Fig. 2 shows the concentration dependence of cell viability for the terpenes of higher and lower cytotoxicity. The IC_{50} values for the eight tested terpenes are presented in Table 1.

3.2. Hemolytic effects of the terpenes

The hemolytic effects of the terpenes on human erythrocytes were evaluated after 1.5 h incubation. Ethanol was used as a vehicle to optimize the incorporation of terpenes into the RBC membranes; the hemolytic effect of ethanol was previously characterized. The levels of ethanol-induced hemolysis measured at 50% hematocrit (Fig. 3A) indicate that damage occurs only at an ethanol concentration above 10% (v/v).

The hemolytic potential can be used to indicate the toxicity of molecules on human erythrocytes (Benavides et al., 2004). In Fig. 3B was plotted the concentration dependence of the most hemolytic terpene (nerolidol) and a less hemolytic terpene (1,8-cineole). Nerolidol is hemolytic at very low concentrations, whereas 1,8-cineole shows significant levels of hemolysis only for concentrations above 10 mM. For the other terpenes used in

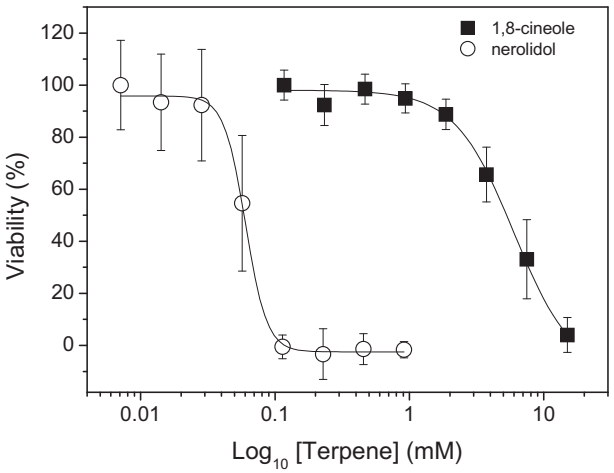

Fig. 2. Balb/c 3T3-A31 NRU cytotoxicity assay after exposing the cells to two representative terpenes for 48 h. Nerolidol and 1,8-cineole were, respectively, the most and the least cytotoxic among the eight tested terpenes. The data represent the mean cell viability ± SD (%) from three independent experiments.

Table 1
IC_{50} values of terpenes obtained from Balb/c 3T3 – A31 NRU cytotoxicity assay after 48 h exposure.

Terpene	IC_{50} (mM)*
Nerolidol	0.06 ± 0.01[a,**]
α-Terpineol	0.13 ± 0.01a
L(−)-carvone	0.93 ± 0.18[b]
Pulegone	1.01 ± 0.21[b]
DL-menthol	1.58 ± 0.26[c]
L-menthone	1.74 ± 0.13[c]
(+)-Limonene	1.58 ± 0.05[c]
1,8-Cineole	4.02 ± 0.15[d]

The means and SD were calculated from three independent experiments.
* In this experiment 1 mM corresponds to 10^{13} terpenes/cell.
** Statistical significance: means that are not marked with the same letter are statistically different at $P < 0.05$ (Tukey test).

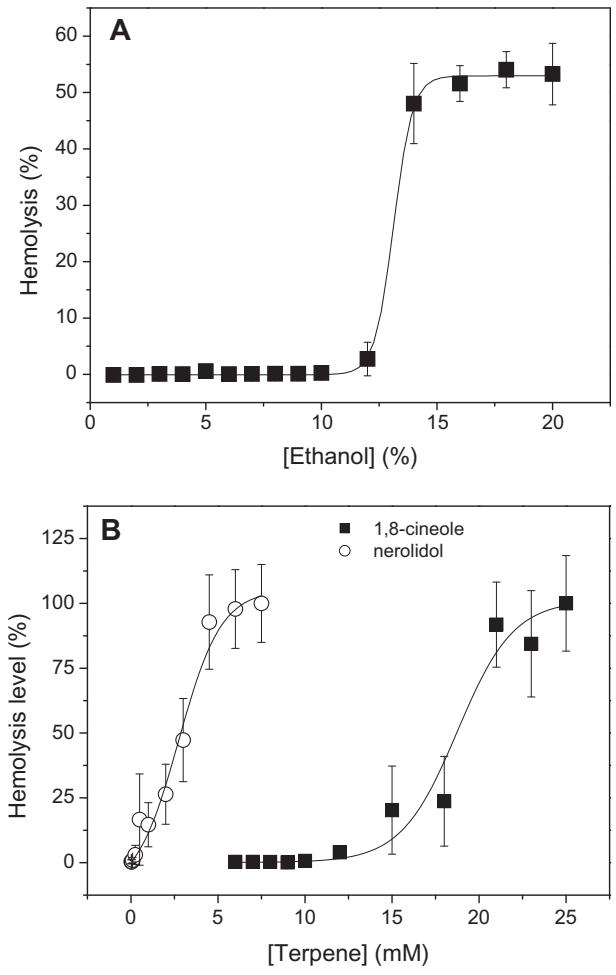

Fig. 3. (A) The hemolysis levels induced after incubating 50% hematocrit erythrocyte suspensions with different ethanol concentrations for 1.5 h. (B) The hemolysis levels induced after incubating 50% hematocrit erythrocyte suspension with different concentrations of nerolidol and 1,8-cineole for 1.5 h.

this work, hemolysis occurs at concentrations between 1.0 and 6.0 mM. The terpene concentration that causes 50% hemolysis was determined based on the sigmoid curve fitting for each molecule, and the values obtained are presented in Table 2.

To examine the potential correlation between the hemolytic effect and the cell viability of fibroblasts exposed to terpenes, the concentration that causes 50% hemolysis for each terpene was plotted against that for IC_{50} (Fig. 4); a weak correlation ($R = 0.61$) was observed.

Table 2
Terpene concentration for 50% hemolysis, after 90 min incubation in RBC suspension.

Terpene	Concentration (mM)	(10^8 terpenes/RBC)
(+)-Limonene	23.8 ± 0.5[a,*]	26.0 ± 0.6
1,8-Cineole	18.4 ± 0.6b	20.1 ± 0.7
L(−)-carvone	10.5 ± 1.4[c]	11.4 ± 1.6
Pulegone	9.6 ± 0.5[c]	10.5 ± 0.6
L-menthone	8.3 ± 0.9[c,d]	9.0 ± 1.0
α-Terpineol	6.1 ± 0.6[d,e]	6.6 ± 0.7
DL-menthol	4.9 ± 1.1[e]	5.3 ± 1.2
Nerolidol	2.3 ± 0.8[f]	2.5 ± 0.9

The means and SD were calculated from three independent experiments.
* Statistical significance: means that are not marked with the same letter are statistically different at $P < 0.05$ (Tukey test).

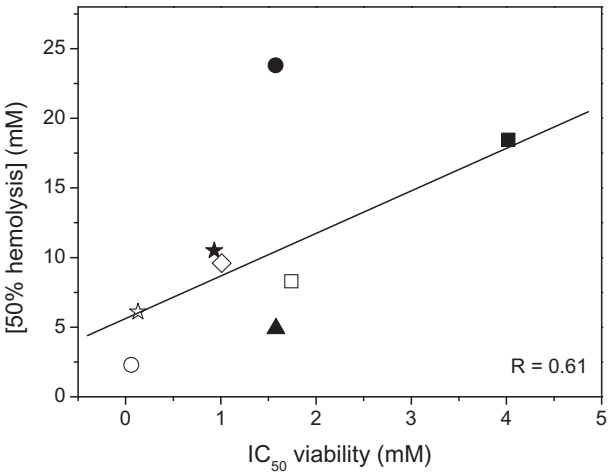

Fig. 4. Correlation between the terpene concentrations required for 50% hemolysis and those needed to obtain the IC_{50} cell viability. Each point in the graph corresponds to one terpene (Tables 1 and 2). Symbols: 1,8-cineole, solid squares; α-terpineol, open stars; DL-menthol, solid triangles; L(−)-carvone, solid stars; (+)-limonene, solid circles; pulegone, open diamonds; L-menthone, open squares; nerolidol, open circles. The value obtained for the correlation coefficient (R) was 0.61.

3.3. Alteration in membrane fluidity

The experimental (black line) and best-fit (red line) EPR spectra 5-DSA in erythrocyte membranes untreated and treated with the terpenes 1,8-cineole and nerolidol are shown in Fig. 5. Spectral simulations allowed us to evaluate the mobility of the spin label in erythrocyte membrane. The experimental line shapes were fitted with the program NLLS using models of one or two spectral components. The presence of two components in the spectra was only observed at high concentrations of some terpenes. The average of τ_c was calculated according to the equation: $\tau_c = N_1 * \tau_{c1} + - N_2 * \tau_{c2}$, where N_1 and N_2 are the population of component 1 and 2, respectively, and τ_{c1} and τ_{c2} are the respective rotation correlation times. The behavior of the τ_c parameter with the terpene concentration in RBC suspension is shown in Fig. 6. Upon nerolidol addition, the τ_c increases significantly until the terpene:cell ratio reaches $\sim 19 \times 10^9$:1. Notably, while the effects of the monoterpenes were similar along the entire concentration range, the sesquiterpene (nerolidol) showed a considerably greater effect, similar to the hemolytic effect and cell viability.

To compare the terpene concentration that causes cytotoxic effects on fibroblasts with terpene concentration that changes membrane fluidity, we performed a measure of fluidity directly on the fibroblast membrane. Fig. 7 shows the EPR spectra and the corresponding values of the rotational correlation time. At a ratio of

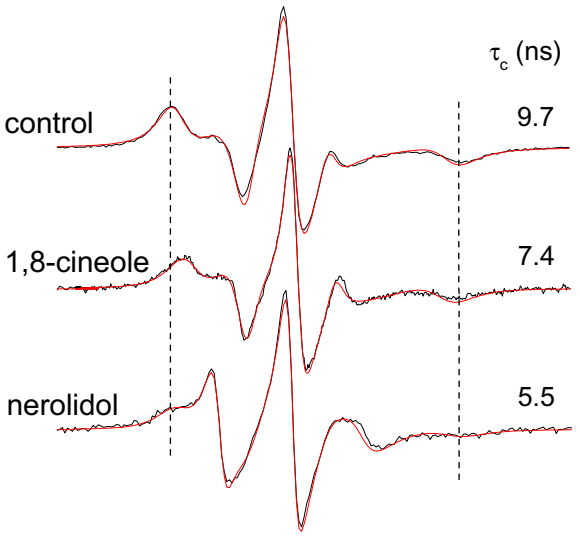

Fig. 5. Experimental (black line) and best-fit (red line) EPR spectra of the 5-DSA in the erythrocyte membranes in the absence of terpenes and after incubating for 90 min with 1,8-cineole or nerolidol at a terpene:cell ratio of 12.7×10^{10}:1 The best-fit spectra were obtained using a NLLS fit with models for one or two spectral components. The values of the EPR parameter rotational correlation time (τ_c) obtained from the fits are indicated. The total scan range of the magnetic field was 100 G. (For interpretation of the references to color in this figure legend, the reader is referred to the web version of this article.)

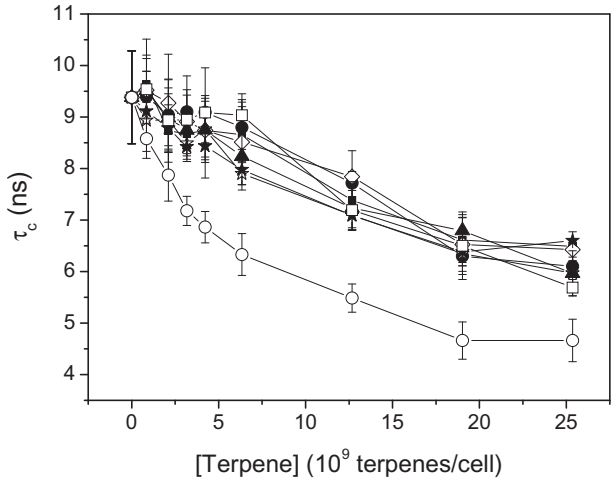

Fig. 6. The rotational correlation time, τ_c, for the 5-DSA within the erythrocyte membranes versus the number of terpenes/erythrocyte. Symbols: 1,8-cineole, solid squares; α-terpineol, open stars; DL-menthol, solid triangles; L(−)-carvone, solid stars; (+)-limonene, solid circles; pulegone, open diamonds; L-menthone, open squares; nerolidol, open circles.

6.3×10^{10}/cell, all terpenes caused strong increases in membrane fluidity, and nerolidol was the most potent. Comparing the τ_c values for the control samples in Figs. 5 and 7, it can be noted that the fibroblast membrane is much more fluid than that of erythrocytes.

4. Discussion

Chemical penetration enhancers are important for use in transdermal drug delivery systems and as components of formulations to enhance topical drug absorption for the treatment of many skin diseases. However, the difficulty of restricting their effects to the outermost stratum corneum layer to avoid irritation or toxicity in deeper skin layers has severely limited their application (Praus-

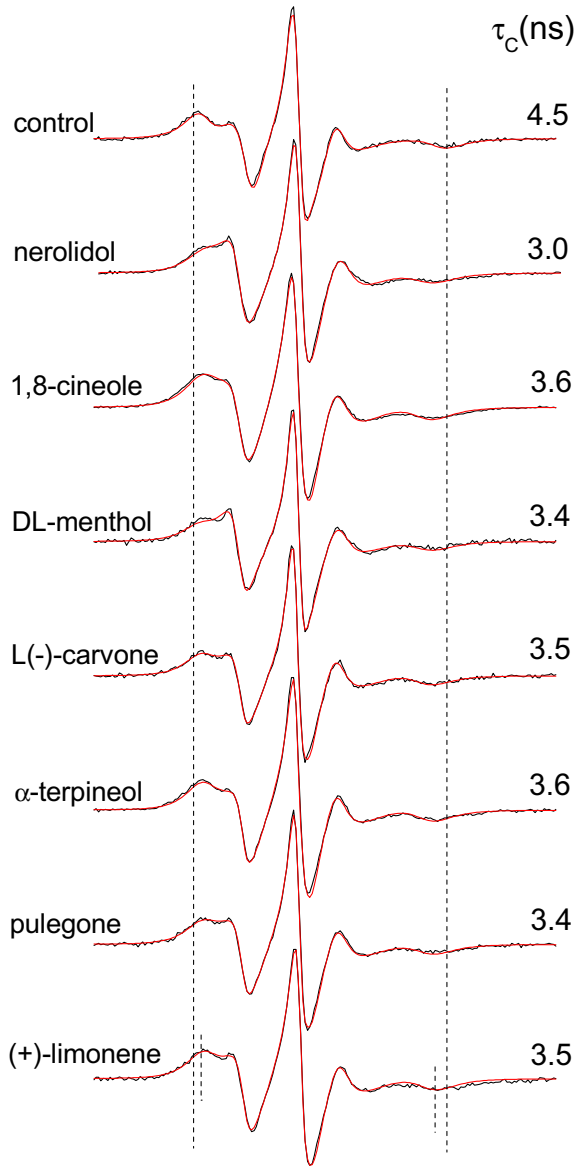

Fig. 7. Experimental (line) and best-fit (circles) EPR spectra of the 5-DSA in the fibroblast membranes for an untreated sample (control) and for fibroblasts treated with several terpenes (90 min incubation) at a terpene:cell ratio of 6.3×10^{10}:1. The best-fit spectra were obtained using a NLLS fit with a model of two spectral components. The values of the EPR parameter rotational correlation time (τ_c) obtained from the fits are indicated. The experimental error is estimated to be 0.2 ns.

nitz and Langer, 2008). It is generally accepted that chemical enhancers might increase the permeability of a drug by affecting the intercellular lipids of the stratum corneum via lipid extraction or fluidization (Barry, 1991; Yamane et al., 1995; Zhao and Singh, 1998). In a study to design skin permeation enhancers in order to optimize the balance between penetration enhancement and low irritation potential, the researchers observed that the use of chemical enhancers as lipid extractors demonstrated a direct correlation between permeability and skin irritation, which was not previously observed for typical fluidizers (Karande et al., 2005). In the present study, we showed that monoterpenes increase the lipid dynamics in the human erythrocyte membrane, but their individual effects are not significantly different. This result is consistent with recently reported data (Dos Anjos et al., 2007; Anjos et al., 2007; Dos Anjos and Alonso, 2008, Camargos et al., 2010), that indicated strong increases of membrane fluidity in stratum

corneum membranes and DPPC vesicles caused by four monoterpenes, but no significant differences were observed between them. Thus, combinations of monoterpenes that facilitate the partition of small drugs with low potential of skin irritation, such as limonene and cineole, with the sesquiterpene nerolidol, which is cytotoxic but has the ability to destabilize the membrane, could be used to achieve the effective permeation of polar and nonpolar drugs through the skin.

As Jain and coworkers (Jain et al., 2002) proposed, terpenes, such as α-terpineol and DL-menthol, which have alcoholic OH groups that act as H-bond donors, could disrupt the existing network of hydrogen bonds within stratum corneum membranes to facilitate the permeation of drugs through the skin. Whereas terpenes, such as menthone, pulegone, carvone and cineole, that only possess hydrogen bond acceptors (carbonyl or ether groups) present a less extensive disruption of the H-bond network and, therefore, show a reduced ability to enhance drug permeation. Similarly, our data showed that the monoterpenes α-terpineol and DL-menthol (H-bond donors) are highly hemolytic; menthone, pulegone, carvone and cineole (acceptors of H-bonds) have moderate hemolytic potential, and limonene, which does not form H-bonds, presented the lowest hemolytic potential. However, the sesquiterpene nerolidol that contained an OH group showed the highest hemolytic and cytotoxic effects. Generally, terpenes might compete with water-mediated intermolecular hydrogen bonding between the lipid molecules, disrupting the hydrogen bond network of the lipid bilayer and weakening the membrane. An important result of this work is that the monoterpenes did not differ significantly in their potency to increase membrane fluidity, but they did differ in their ability to disrupt the erythrocyte membrane (Table 2) and to cause cytotoxicity in fibroblasts (Table 1). The less polar monoterpenes, limonene and cineole, showed less aggression to the membrane and low cytotoxicity. Nerolidol showed greater potency to increase membrane fluidity but also increased ability to disrupt the membrane and increased cytotoxic potential.

The nerolidol concentration that caused 50% hemolysis was approximately 2.5×10^8 molecules/cell (Table 2), whereas the concentration that produced a significant increase in erythrocyte membrane fluidity was 2.5×10^9 molecules/cell. Thus, the change in membrane fluidity was observed at a concentration 10 times greater than that for hemolysis. This result could be explained by the fact that the spin probes are sparsely distributed in the membrane and, therefore, the spin probe spectroscopy only detects changes in fluidity when a widespread change occurs in the membrane. The molar ratio between spin probe and lipid present in the membranes used for the EPR measurements was 1:200. Thus, to detect changes in membrane fluidity, the environment of most spin labels would have to be changed. This result also suggests that a highly localized change in the erythrocyte membrane is sufficient to provoke hemolysis. In cell cytotoxicity, the IC_{50} of nerolidol was 6×10^{11} molecules/fibroblast and the concentration that alters fibroblast membrane fluidity was approximately 10 times lower (6.3×10^{10} terpenes/cell). These calculations indicate that the concentrations that cause a general change in fibroblast membrane fluidity are smaller than those that inhibit the growth of fibroblasts. This result is indicative of the low toxicity of terpenes in cultured fibroblasts and suggests that, unlike in red blood cells, change in fibroblast membrane fluidity occurs without disruption of the membrane.

In conclusion, we examined the hemolytic potential and cytotoxicity in fibroblasts treated with terpenes and showed that these reagents cause cellular injury in a concentration-dependent manner. Nerolidol, α-terpineol and DL-menthol were the most hemolytic and limonene and 1,8-cineole were the least hemolytic, whereas in the cytotoxicity assay, nerolidol and α-terpineol were the most cytotoxic and 1,8-cineole was the least cytotoxic; however, the correlation coefficient between the two tests was low ($R = 0.61$). This study demonstrated that monoterpenes are powerful membrane fluidizers in erythrocyte and fibroblast cells, and the observed effects were not significantly different among them, suggesting that they possess the same potency in enhancing dermal permeation. However, less polar monoterpenes, such as limonene and cineole, showed low membrane aggressiveness and cytotoxicity. The sesquiterpene produced the greatest increase in membrane fluidity, but also a greater irritation potential. Although the mechanisms of cytotoxicity were not investigated, we suggest that terpenes could trigger various mechanisms, including interactions with the cellular membrane, which most likely occur during terpene-induced hemolysis. The antiproliferative effects of monoterpenes have been previously demonstrated through the modulation of gene expression associated with apoptosis (Bardon et al., 1998, 2002; Yang and Ping Dou, 2010; Wu et al., 2012). Given that some monoterpenes show activity against Leishmania infantum promastigotes (Morales et al., 2009) and the sesquiterpene nerolidol inhibits the growth of several species of Leishmania promastigotes and amostigotas (Arruda et al., 2005), these reagents are interesting candidates as components of formulations for the topical treatment of cutaneous Leishmania. In this case, the terpenes or their combinations would not only serve as chemical permeation enhancers of drugs with antileishmanial activity but could also contribute to the antiparasitic treatment.

Acknowledgments

This work was financially supported through grants from the Brazilian research funding agencies CNPq, CAPES, FUNAPE and FAPEG. The authors are grateful to the Goiano Institute of Oncology and Hematology (INGOH) and Hemolabor – clinical analysis laboratories for supplying the blood used in this study. Sebastião A. Mendanha, Jorge L.V. Anjos and Soraia S. Moura are recipients of fellowships from CAPES. Marize C. Valadares and Antonio Alonso are recipients of research grants from the CNPq.

References

Alonso, A., Santos, W.P., Leonor, S.J., Santos, J.G., Tabak, M., 2001. Stratum corneum protein dynamics as evaluated by a spin label maleimide derivative. Effect of urea. Biophys. J. 81, 3566–3576.

Alonso, A., Silva, J.V., Tabak, M., 2003. Hydration effects on the protein dynamics in stratum corneum as evaluated by EPR spectroscopy. Biochim. Biophys. Acta 1646, 32–41.

Anjos, J.L.V.d., Neto, D.dS., Alonso, A., 2007. Effects of 1,8-cineole on the dynamics of lipids and proteins of stratum corneum. Int. J. Pharm. 345, 81–87.

Arruda, D.C., D'Alexandri, F.L., Katzin, A.M., Uliana, S.R.B., 2005. Antileishmanial activity of the terpene nerolidol. Antimicrob. Agents Chemother. 49, 1679–1687.

Bardon, S., Picard, K., Martel, P., 1998. Monoterpenes inhibit cell growth, cell cycle progression and cyclin D1 gene expression in human breast cancer cell lines. Nutr. Cancer 32, 1–7.

Bardon, S., Foussard, V., Fournel, S., Loubat, A., 2002. Monoterpenes inhibit proliferation of human colon cancer cells by modulating cell cycle-related protein expression. Cancer Lett. 181, 187–194.

Barry, B.W., 1991. Lipid-Protein-Partitioning theory of skin penetration enhancement. J. Control. Release 15, 237–248.

Benavides, T., Mitjans, M., Martínez, V., Clapés, P., Infante, M.R., Clothier, R.H., Vinardell, M.P., 2004. Assessment of primary eye and skin irritants by in vitro cytotoxicity and phototoxicity models: an in vitro approach of new arginine-based surfactant-induced irritation. Toxicology 197, 229–237.

Budil, D.E., Lee, S., Saxena, S., Freed, J.H., 1996. Nonlinear-least-squares analysis of slow-motional EPR spectra in one and two dimensions using a modified Levenberg–Marquardt algorithm. J. Magn. Reson. A 120, 155–189.

Camargos, H.S., Silva, A.H.M., Anjos, J.L.V., Alonso, A., 2010. Molecular dynamics and partitioning of di-tert-butyl nitroxide in stratum corneum membranes: effect of terpenes. Lipids 45, 419–427.

Cornwell, P.A., Barry, B.W., 1994. Sesquiterpene components of volatile oils as skin penetration enhancers for the hydrophilic permeant 5-fluorouracil. J. Pharm. Pharmacol. 46, 261–269.

Crowell, P.L., 1999. Prevention and therapy of cancer by dietary monoterpenes. J. Nutr. 129, 775S–778S.

Dos Anjos, J.L.V., Alonso, A., 2008. Terpenes increase the partitioning and molecular dynamics of an amphipathic spin label in stratum corneum membranes. Int. J. Pharm. 350, 103–112.

Dos Anjos, J.L.V., Neto, D.D., Alonso, A., 2007. Effects of ethanol/L-menthol on the dynamics and partitioning of spin-labeled lipids in the stratum corneum. Eur. J. Pharm. Biopharm. 67, 406–412.

El-Kattan, A.F., Asbill, C.S., Michniak, B.B., 2000. The effect of terpene enhancer lipophilicity on the percutaneous permeation of hydrocortisone formulated in HPMC gel systems. Int. J. Pharm. 198, 179–189.

Gould, M.N., 1997. Cancer chemoprevention and therapy by monoterpenes. Environ. Health Perspect. 105 (Suppl. 4), 977–979.

Jain, A.K., Thomas, N.S., Panchagnula, R., 2002. Transdermal drug delivery of imipramine hydrochloride. I: Effect of terpenes. J. Control. Release 79, 93–101.

Karande, P., Jain, A., Ergun, K., Kisperky, V., Mitragotri, S., 2005. Design principles of chemical penetration enhancers for transdermal drug delivery. Proc. Natl. Acad. Sci. USA 102, 4688–4693.

Kitahara, M., Ishiguro, F., Takayama, K., Isowa, K., Nagai, T., 1993. Evaluation of skin damage of cyclic monoterpenes, percutaneous absorption enhancers, by using cultured human skin cells. Biol. Pharm. Bull. 16, 912–916.

McGarvey, D.J., Croteau, R., 1995. Terpenoid metabolism. Plant Cell 7, 1015–1026.

Morales, M., Navarro, M.C., Martin, J., Valero, A., Lara, A.M., Barón, S., Morillas, F., 2009. Activity of different monoterpenic derivatives of natural origin against Leishmania infantum promatisgotes. Rev. Ibero-latinoam. Parasitol. 68, 65–72.

Morimoto, H., Wada, Y., Seki, T., Sugibayashi, K., 2002. In vitro skin permeation of morphine hydrochloride during the finite application of penetration-enhancing system containing water, ethanol and l-menthol. Biol. Pharm. Bull. 25, 134–136.

Oliva, B., Piccirilli, E., Ceddia, T., Pontieri, E., Aureli, P., Ferrini, A.M., 2003. Antimycotic activity of Melaleuca alternifolia essential oil and its major components. Lett. Appl. Microbiol. 37, 185–187.

Polo, M.P., de Bravo, M.G., 2006. Effect of geraniol on fatty-acid and mevalonate metabolism in the human hepatoma cell line Hep G2. Biochem. Cell Biol. 84, 102–111.

Prausnitz, M.R., Langer, R., 2008. Transdermal drug delivery. Nat. Biotechnol. 26, 1261–1268.

Queirós, W.P., Neto, D.S., Alonso, A., 2005. Dynamics and partitioning of spin-labeled stearates into the lipid domain of stratum corneum. J. Control. Release 106, 374–385.

Rabi, T., Bishayee, A., 2009. Terpenoids and breast cancer chemoprevention. Breast Cancer Res. Treat. 115, 223–239.

Schneider, D.J., Freed, J.H., 1989. Biological magnetic resonance. In: Berliner, L.J., Reuben, J. (Eds.), Spin labeling: Theory and Application. Plenum Press, New York, pp. 1–76.

Thoppil, R.J., Bishayee, A., 2011. Terpenoids as potential chemopreventive and therapeutic agents in liver cancer. World J. Hepatol. 27, 228–249.

Vaddi, H.K., Ho, P.C., Chan, S.Y., 2002. Terpenes in propylene glycol as skin-penetration enhancers: permeation and partition of haloperidol, Fourier transform infrared spectroscopy, and differential scanning calorimetry. J. Pharm. Sci. 91, 1639–1651.

Wu, C.S., Chen, Y.J., Chen, J.J., Shieh, J.J., Huang, C.H., Lin, P.S., Chang, G.C., Chang, J.T., Lin, C.C., 2012. Terpinen-4-ol induces apoptosis in human nonsmall cell lung cancer in vitro and in vivo. Evid. Based Complement. Alternat. Med. 818261, 13.

Yamane, M.A., Williams, A.C., Barry, B.W., 1995. Effects of terpenes and oleic acid as skin penetration enhancers towards 5-fluorouracil as assessed with time; permeation, partitioning and differential scanning calorimetry. Int. J. Pharm. 116, 237–251.

Yang, H., Ping Dou, Q., 2010. Targeting apoptosis pathway with natural terpenoids: Implications for treatment of breast and prostate cancer. Curr. Drug Targets 11, 733–744.

Zhao, K., Singh, J., 1998. Mechanisms of percutaneous absorption of tamoxifen by terpenes: eugenol, D-limonene and menthone. J. Control. Release 55, 253–260.